

# Optimal connection of wind turbines to distribution grid to minimize power loss

Dinh Chung Phan, Ngoc An Luu

Faculty of Electrical Engineering, The University of Danang, University of Science and Technology, Danang City, Vietnam

## Article Info

### Article history:

Received Feb 19, 2022

Revised Aug 10, 2022

Accepted Aug 25, 2022

### Keywords:

Algorithm  
Distribution grid  
Loss minimization  
Operation mode  
Wind turbine

## ABSTRACT

This research aims to connect wind turbines to a distribution grid to minimize the power loss and to satisfy the grid's normal operating condition. The proposed algorithm will determine optimal positions, optimal operation mode and wind turbine type. We must choose the best operation mode from available modes including the constant power factor mode and the constant voltage mode. According to the optimal operation mode, we decide the optimal setting data of wind turbine. This algorithm is coded in MATLAB software and implemented to IEEE 33-buses distribution grid. Noted that in this research, we tested two cases including the original IEEE 33-buses grid and its modification where the power system connected to this grid at multi-position. Results indicated that the proposed algorithm could determine the number of wind turbines, position, optimal operation mode, wind turbine type and the priority order of wind turbine installation to minimize power loss. Moreover, results were also compared to that of other algorithms.

*This is an open access article under the [CC BY-SA](#) license.*



## Corresponding Author:

Dinh Chung Phan

Faculty of Electrical Engineering, The University of Danang, University of Science and Technology

54 Nguyen Luong Bang Street, Danang City, Vietnam

Email: pdchung@dut.udn.vn

## 1. INTRODUCTION

Renewable energy resources have been considered and exploited in many countries in the world; they have contributed an essential part of demand [1]. For solar energy, solar farms are in the range of several kW to MW, and hence, it can integrate to distribution grids quite conveniently. Unlikely, the wind turbine (WT) rating is often several ten kW to MW and wind plants are often connected to transmission grid [2]. However, in areas with low wind potential, we only use small WTs, and they are connected to distribution grids.

For distribution grids, the high-power loss and low node voltage are serious issues [3]. To improve these problems, distributed generators (DG) are recommended to install in the distribution grid. However, determining the optimal position to install is an important issue, and until now, many methods were proposed to tackle this problem [4]–[20]. These methods can be generally divided into three groups. The first group took the economic problem into account [4]–[11]; most research focused on the minimal active power loss [4]–[11] and the maximal electrical energy capture [10]; some of them, authors took the cost and profit maximization into account [10]. The second group concerns technical issues like power quality, stability, and so on [10]–[12]; some research focused on the voltage stability improvement [10]–[12]. The final group considers multi-objective [14]–[20]; at least two objectives from the technique and economic issues is expected to obtain; in this group, the combination of optimal power loss and voltage stability is well-known [15]–[20]. Generally, authors mainly focused on algorithms to obtain the cost function and they did not consider the type of DG (WT, diesel or photovoltaic); the DG unit in these studies often operates in either

power quality (PQ) mode or photovoltaic (PV) mode, and authors did not consider which the operation mode is the best [5], [12]. Moreover, the DG units' rating is normally an available value, for example 100 kW, 160 kW, 200 kW, and hence, the DGs' size determined by algorithms is often different from available sizes and we must choose an approximate size; this can make the cost function fail.

In terms of WT, WTs are classified into two groups including fixed speed wind turbine (FSWT) and variable speed wind turbine (VSWT) [21]. For FSWT, it consumes the reactive power from the grid because it is connected directly to the grid [21], and this can make the power loss of the grid increase. For VSWT, if a doubly feed induction generator (DFIG) is used, a power converter with 30% of the DFIG capacity must be installed in the rotor side [21]; and hence, the DFIG turbine is named partial-power-converter based WT (PCWT); by contrast, in the case of a synchronous generator, the converter rating is the same as the generator rating, and hence, it is called full power converter based WT (FCWT) [21]; a VSWT can operate in either the constant voltage mode (CVM) or the constant power factor mode (CPFM) [21]; and noted that the reactive power capacity limitation of PCWT is different from that of FCWT [22]. Practically, VSWT can withdraw a higher energy than FSWT. Hence, in this research, we only use VSWT, and we consider both VSWT type and its operation mode.

This research's objective is to minimize the power loss of a distributed grid by using VSWT. Firstly, we will determine the optimal position where the wind turbine is connected; secondly, the VSWT type, optimal operation mode (OOM) and setting parameters of each VSWT are suggested. The proposed algorithm is coded in MATLAB, and we will test two cases of IEEE 33-bus grid including the original IEEE 33-bus grid and its modification that multi-nodes are connected to the power system. Results are analyzed and compared to those without WTs, and we also compare these results to that of some previous methods.

## 2. ALGORITHM OF OPTIMAL WIND TURBINE CONNECTION IN A DISTRIBUTION GRID

To reduce the power loss in a distribution grid, we can install WTs to supply the power to local loads. Here, WT installation must ensure that the power loss in the grid in total,  $\Delta P$ , is minimum, and constraints including the nodes' voltage limitation and all lines' overload condition are satisfied. Hence, the cost function and constraints are described as (1)-(3),

$$\Delta P = \sum_{q=1}^m \Delta p_q \rightarrow \text{minimize} \quad (1)$$

with constraints

$$V_{min} \leq V_i \leq V_{max} \quad (2)$$

$$I_{ij} \leq I_{ij,max} \quad (3)$$

where,  $m$  is the number of lines in the grid;  $\Delta p_q$  is the power loss on the  $q^{th}$  line;  $V_i$  is the voltage at the  $i^{th}$  node;  $I_{ij}$  and  $I_{ij,max}$  are the current on the line, connecting between the  $i^{th}$  node and the  $j^{th}$  node, and its load capacity; and  $V_{min}$  and  $V_{max}$  are the voltage limitations at the  $i^{th}$  node. To obtain the power loss minimization (PLM), we propose an algorithm to determine the number, position, operation mode, and type of WT as Figure 1.

### 2.1. Main algorithm

The idea of this algorithm is step by step increase in the WT number to determine the optimal connection of each WT. It means we determine the optimal position, OOM, and WT type based on (1)-(3); when the optimal position of the first WT was determined, we suppose that the first WT is already connected to that position, and the next, we consider the second WT; this is repeated until all WTs ( $n_{WT,max}$ ) are considered. When all WTs have been considered, we decide the optimal WT number. This algorithm, Figure 1(a), is explained as:

- Step 1: reading the grid's data including the node type, magnitude and phase angle of voltage buses, load power, the generation power and its reactive power limitation at nodes, lines' impedance, line's capacity, and so on. The set of all parameters is named *Data*. In this step, we use Newton Raphson method to determine  $\Delta P$ , and the minimum voltage,  $V_{min}^b$ , in the base case which WTs have not yet connected to the grid. After running the base case, we set  $k = 1$ ,  $V_{min}^{k-1} = V_{min}^b$ , and  $Data^{k-1} = Data$ . Here,  $k$  is the  $k^{th}$  WT corresponding to the  $k^{th}$  stage and  $V_{min}^{k-1}$  is the minimum voltage in this grid in the  $k^{th}$  stage.

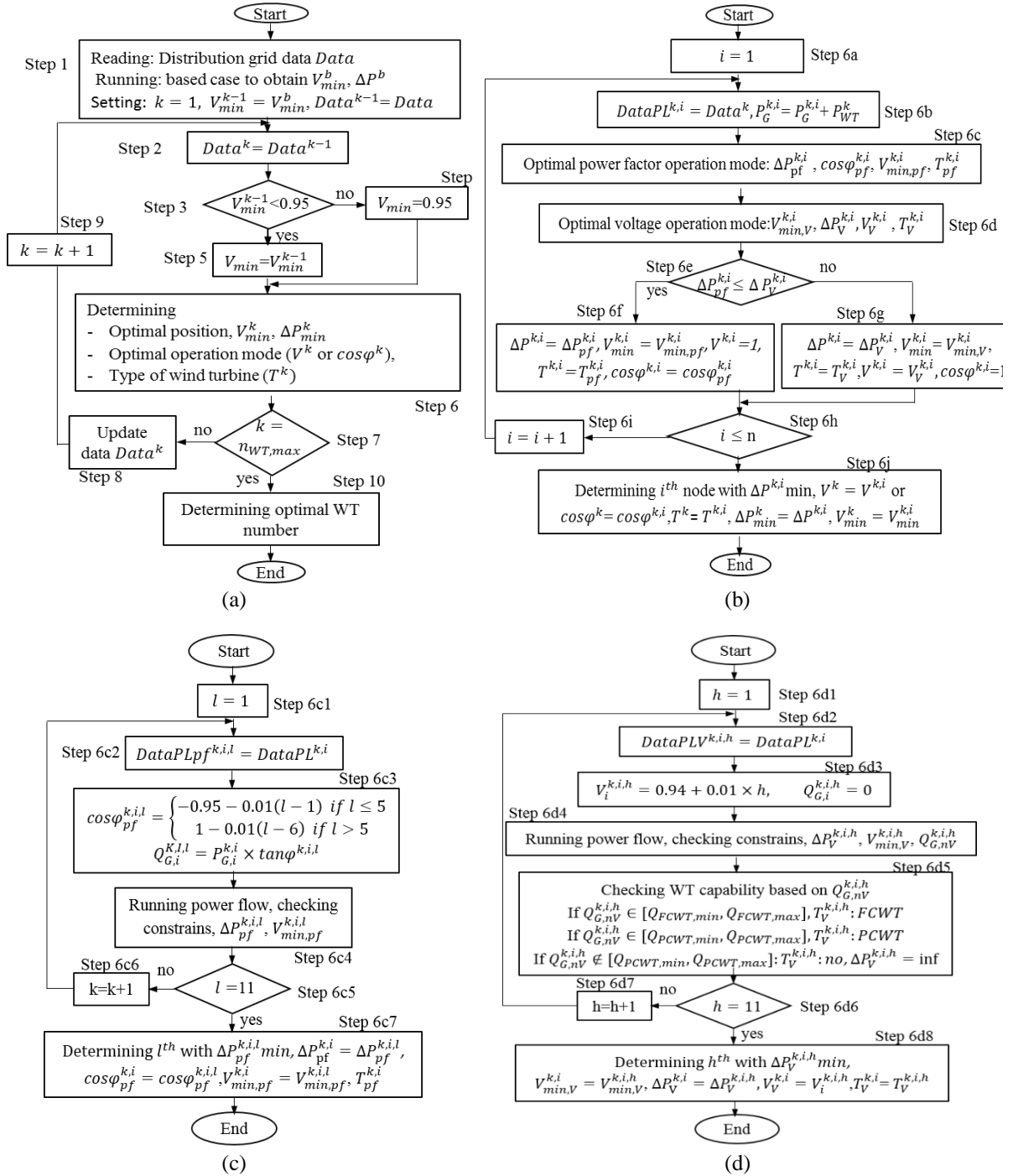


Figure 1. PLM algorithms (a) general algorithm, (b) OOM, (c) CPFM, and (d) CVM

- Step 2: setting the data of the distribution grid  $Data^k = Data^{k-1}$ .
- Step 3: checking the minimum voltage  $V_{min}^{k-1}$ . If  $V_{min}^{k-1} \geq 95\%$ , we go to Step 4, otherwise, we go to Step 5.
- Step 4: setting  $V_{min} = 95\%$  of the rated value,  $V_{rated}$ , and going to Step 6.
- Step 5: setting  $V_{min} = V_{min}^{k-1}$  and going to Step 6.
- Step 6: determining the optimal position, OOM and type of the  $k^{th}$  WT. Assuming that  $\Delta P^k$  is minimum when the  $k^{th}$  WT is connected to the  $j^{th}$  node. Hence, we obtain the optimal position ( $j^{th}$ );  $V_{min}^k, \Delta P^k$ ; OOM ( $V^k$  or  $\cos\phi^k$ ), and WT type ( $T^k$ ). For more detail, we can refer to Figure 1(b) and Subsection 2.2.
- Step 7: checking the condition of  $k$ . If  $k = n_{WT,max}$ , we go to Step 10, otherwise, Step 8 is done.

- Step 8: updating data: assuming that the  $k^{th}$  WT optimal position is the  $j^{th}$  node, we update the generated active power at the  $j^{th}$  node ( $P_{G,j}^k$ ) as  $P_{G,j}^k = P_{G,j}^{k-1} + P_{wt}^k$ . If OOM is CPFM, the type of  $j^{th}$  node is PQ node, the reactive power  $Q_{G,j}^k = P_{G,j}^k \tan \varphi^k$ , the voltage  $V_j^k$  at the  $j^{th}$  node  $V_j^k = 1 pu$ , and the WT type at the  $k^{th}$  stage is PCWT or FCWT. If OOM is CVM, the type of  $j^{th}$  node is PV node,  $Q_{G,j}^k = 0$ ,  $V_j^k = V^k$ , the type of WT:  $T^k$ .
- Step 9: moving to the  $(k + 1)^{th}$  WT and then return to Step 2.
- Step 10: determining the number and position of WTs based on  $\min\{\Delta P^k, \Delta P^k, \dots, \Delta P^{n_{WT,max}}\}$ .

## 2.2. Algorithm determining the optimal operation mode (OOM)

This algorithm, Figure 1(b), aims to determine OOM of the  $k^{th}$  WT if it is connected to the  $i^{th}$  node. Here, we compare the power loss in total of the grid as WTs at the  $i^{th}$  node in CPFM,  $\Delta P_{pf}^{k,i}$ , to that in CVM,  $\Delta P_V^{k,i}$ . For CPFM, we must obtain the optimal power factor  $\cos \varphi^{k,i}$  as the algorithm in Figure 1(c). For CVM, we must obtain the optimal voltage  $V^{k,i}$  and the WT type  $T^{k,i}$  as the algorithm in Figure 1(d). Noted that if the  $k^{th}$  WT operates in the power factor mode,  $T^{k,i}$  can be set either PCWT or FCWT. The algorithm's outputs consist of OOM, the power loss  $\Delta P_{min}^k$ , the minimum voltage  $V_{min}^k$ , and the  $k^{th}$  WT type,  $T^{k,i}$ . This algorithm is described as:

- Step 6a: starting the first node in the list of load node  $i = 1$ .
- Step 6b: using  $DataPL^{k,i}$  to calculate and choose OOM as the  $k^{th}$  WT connected to the  $i^{th}$  node. Here, we set  $DataPL^{k,i} = DataPL^k$  and update the generation power at the  $i^{th}$  node  $P_{G,i}^{k,i} = P_{G,i}^{(k-1),i} + P_{wt}^k$ .
- Step 6c: using  $DataPL^{k,i}$  to determine the optimal power factor of this WT. In this step, we obtain  $\Delta P_{pf}^{k,i}$ ,  $\cos \varphi^{k,i}$ ,  $V_{min,pf}^{k,i}$ ,  $T_{pf}^{k,i}$ . The detail of this step is described in Figure 1(c).
- Step 6d: using  $DataPL^{k,i}$  to determine the optimal voltage of this WT. In this step, we obtain  $\Delta P_V^{k,i}$ ,  $V_V^{k,i}$ ,  $V_{min,V}^{k,i}$ ,  $T_V^{k,i}$ . The detail of this step is described in Figure 1(d).
- Step 6e: comparing  $\Delta P_{pf}^{k,i}$  and  $\Delta P_V^{k,i}$ . If  $\Delta P_{pf}^{k,i} \leq \Delta P_V^{k,i}$ , we move to Step 6f, otherwise, we move to Step 6g.
- Step 6f: setting  $\Delta P^{k,i} = \Delta P_{pf}^{k,i}$ ,  $V_{min}^{k,i} = V_{min,pf}^{k,i}$ ,  $\cos \varphi^{k,i} = \cos \varphi_{pf}^{k,i}$ ,  $V^{k,i} = 1$ ,  $T^{k,i} = T_{pf}^{k,i}$ .
- Step 6g: setting  $\Delta P^{k,i} = \Delta P_V^{k,i}$ ,  $V_{min}^{k,i} = V_{min,V}^{k,i}$  and parameters concerning to this mode is  $T^{k,i} = T_V^{k,i}$ ,  $\cos \varphi^{k,i} = 1$ , and  $V^{k,i} = V_V^{k,i}$ .
- Step 6h: comparing  $i$  and load node number,  $n$ . If  $i < n$ , we move to Step 6i. Otherwise, we move to Step 6j.
- Step 6i: moving to next load node and then, returning to Step 6b.
- Step 6j: choosing the  $i^{th}$  node, where  $\Delta P^{k,i} = \min\{\Delta P^{k,1}, \Delta P^{k,2}, \dots, \Delta P^{k,n}\}$ , is the optimal position and other parameters such as OOM, the WT type, the minimum voltage in this grid are determined according to the  $i^{th}$  node. Hence, we set  $V^k = V^{k,i}$ ,  $T^k = T^{k,i}$ ,  $\cos \varphi^k = \cos \varphi^{k,i}$ ,  $\Delta P_{min}^k = \Delta P^{k,i}$ ,  $V_{min}^k = V_{min}^{k,i}$ . We finish this algorithm.

## 2.3. Algorithm determining the optimal power factor mode

The algorithm described in Figure 1(c) is to decide the optimal power factor of the  $k^{th}$  WT connecting to the  $i^{th}$  node. By varying the power factor from +95% to -95% [23] with 10% each step, we run Newton Raphson program to decide the optimal power factor based on PLM. This algorithm is described as:

- Step 6c1: setting  $l = 1$ .
- Step 6c2: defining a new set of data,  $DataPLpf$ , to calculate in the case of the  $k^{th}$  WTs at the  $i^{th}$  node in CPFM. Here, we set  $DataPLpf^{k,i,l} = DataPL^{k,i}$ .
- Step 6c3: computing the power factor and reactive power of the  $k^{th}$  WT at the  $i^{th}$  node as

$$\begin{aligned} \cos \varphi^{k,i,l} &= (-0.95 - 0.1(l - 1)) \quad \text{if } l \leq 5 \\ \cos \varphi^{k,i,l} &= (1 - 0.1(l - 6)) \quad \text{if } l > 5 \\ Q_{G,i}^{k,i,l} &= P_{G,i}^k \tan \varphi^{k,i,l}. \end{aligned}$$

- Step 6c4: running Newton Raphson program and checking constrains (2)-(3). If all constrains are satisfied, we obtain  $\Delta P_{pf}^{k,i,l}$  and  $V_{min,pf}^{k,i,l}$ . If one of these constraints is violated, we can set  $\Delta P^{k,i,l} = inf$ .
- Step 6c5: checking  $l$  value. If  $l = 11$ , we move to Step 6c6. Otherwise, we move to Step 6c7.

- Step 6c6: increasing  $l$  to  $l = l + 1$  and then, we return Step 6c2.
- Step 6c7:  $\cos\varphi_{pf}^{k,i,l}$  is the optimal value if  $\Delta P_{pf}^{k,i,l} = \min\{\Delta P_{pf}^{k,i,1}, \Delta P_{pf}^{k,i,2}, \dots, \Delta P_{pf}^{k,i,11}\}$ , and here, we set  $\cos\varphi_{pf}^{k,i} = \cos\varphi_{pf}^{k,i,l}$ ,  $\Delta P_{pf}^{k,i} = \Delta P_{pf}^{k,i,l}$ ,  $V_{min,pf}^{k,i} = V_{min,pf}^{k,i,l}$ ,  $V_{pf}^{k,i} = 1$ ,  $T_{pf}^{k,i,l}$  can be set either PCWT or FCWT. We finish this algorithm.

#### 2.4. Algorithm determining the optimal voltage mode

This algorithm, shown in Figure 1(d), determine the optimal voltage at the  $i^{th}$  node where the  $k^{th}$  WT is connected. Here, we change step by step the voltage at this  $i^{th}$  node from 95% to 105% of the rated value to determine the optimal voltage value that we obtain PLM. From the required reactive power and WT's reactive power capability at PV nodes, we determine WT type. This algorithm is described as

- Step 6d1: setting  $h = 1$ .
- Step 6d2: defining a new data set,  $DataPLV$ , for CVM and setting  $DataPLV^{k,i,h} = DataPL^{k,i}$
- Step 6d3: setting the voltage value and reactive power at the  $i^{th}$  node  $V_i^{k,i,h} = 0.94 + 0.01h$ , and  $Q_{G,i}^{k,i,h} = 0$ .
- Step 6d4: running the Newton Raphson program and checking constraint conditions (2)-(3). If all constraints are satisfied, we calculate  $\Delta P_V^{k,i,h}$ ,  $V_{min,V}^{k,i,h}$ , the reactive power of WTs at all PV nodes  $Q_{G,nV}^{k,i,h}$  ( $Q_{G,nV}^{k,i,h} = \{Q_{G,V1}^{k,i,h}, Q_{G,V2}^{k,i,h}, \dots, Q_{G,Vv}^{k,i,h}\}$ ). If one of these constraints is violated, we set  $\Delta P_V^{k,i,h} = inf$ .
- Step 6d5: checking the WT reactive power capability and  $Q_{G,nV}^{k,i,h}$ . If  $Q_{FCWT,min}^{k,i,h} \leq Q_{G,nV}^{k,i,h} \leq Q_{FCWT,max}^{k,i,h}$ , the type of WT at the  $v^{th}$  node ( $T^{k,i,h}$ ) is FCWT. Otherwise, if  $Q_{PCWT,min}^{k,i,h} \leq Q_{G,nV}^{k,i,h} \leq Q_{PCWT,max}^{k,i,h}$ , the type of WTs at  $v^{th}$  node is PCWT. If above conditions are failed, we set  $\Delta P_V^{k,i,h} = inf$ .
- Step 6d6: checking the voltage condition. If  $V_i^{k,i,h} < 1.05$ , we move to Step 6d7, otherwise, Step 6d8 is done.
- Step 6d7: increasing  $h$  to  $h = h + 1$  and return to Step 6d2.
- Step 6d8: determining the  $V_i^{k,i,h}$  is the optimal voltage if  $\Delta P_V^{k,i,h} = \min\{\Delta P_V^{k,i,1}, \Delta P_V^{k,i,2}, \dots, \Delta P_V^{k,i,11}\}$ . We set  $\Delta P_V^{k,i} = \Delta P_V^{k,i,h}$ ,  $V_{min,V}^{k,i} = V_{min,V}^{k,i,h}$ ,  $V^{k,i} = V_i^{k,i,h}$ ,  $T^{k,i} = T_V^{k,i,h}$ .
- This algorithm is finished.

### 3. RESULTS AND DISCUSSION

To test the proposed algorithm, the IEEE 33-bus distribution grid as Figure 2 is used. In this figure, the grid with continuous line is the original IEEE 33-bus distribution grid [24] while that with dotted line is the modified configuration of this grid. The structure and parameters of the modified IEEE 33-bus distribution grid is completely the same as the original case; the different point is that the modified grid is connected to the power system at multi nodes as the discontinuous line. Noted that the parameters of the original IEEE 33-bus grid data are taken from [24] and each WT in this research is 100 kW [25]. With the parameters of 100 kW WT [26], the reactive power range of PCWT is approximate to from -80 to 75 kVAr while that of FCWT is from -40 to 40 kVAr.

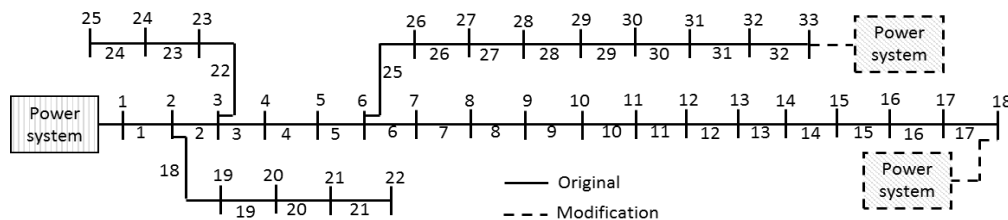


Figure 2. Original IEEE 33-bus distribution grid

#### 3.1. Original IEEE 33-bus distribution grid

We suppose that the 1st node is connected to the power grid and its voltage is always remained at 12.66 kV (the rated value). By running the proposed algorithm, results are shown in Table 1. As can be seen from Table 1, to minimize the power loss in the original IEEE 33-bus distribution grid, we must install 32 WTs of 100 kW at 15 nodes. The node requiring the highest number of WTs (9 WTs) is the 30<sup>th</sup> node; the

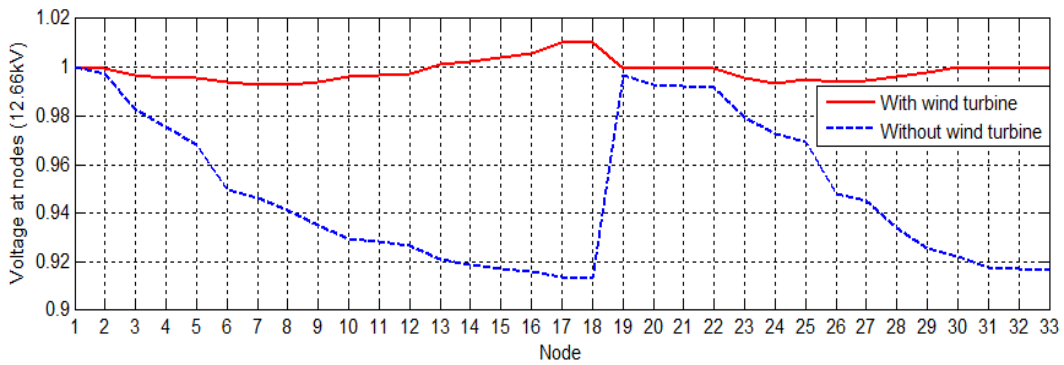
next node is the 25<sup>th</sup> node, the 17<sup>th</sup> node, and the 32<sup>nd</sup> node with 6, 4, and 2 WTs, respectively; for the other 11 nodes, we only install 1 WT for each node. Concerning to OOM, WTs at three nodes including the 17<sup>th</sup> node, 25<sup>th</sup> node, and 30<sup>th</sup> node must operate in CVM; and the voltage at these nodes is always kept at 101%, 99.5% and 100%, respectively; WTs at other nodes must operate in the CPFM with the power factor of 95%. This table also indicates that only WTs at the 25<sup>th</sup> node and the 30<sup>th</sup> node must employ PCWT whereas other nodes, WT can be either FCWT or PCWT.

Table 1. Location, operation mode and type of WT in the original IEEE 33-bus distribution grid

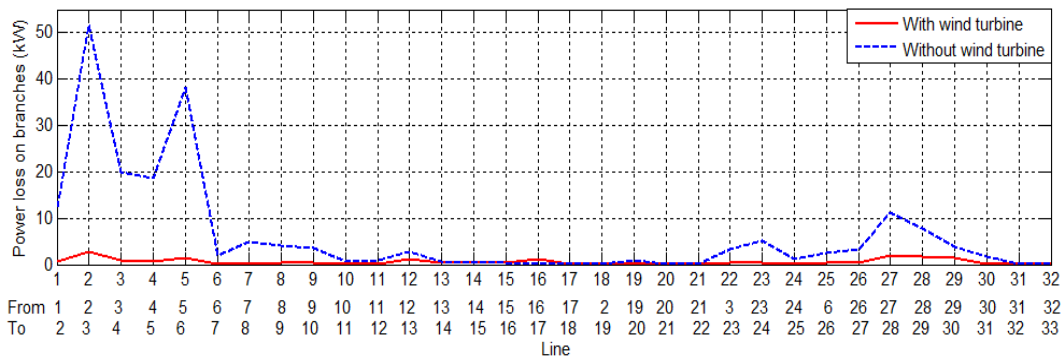
Node	11 <sup>th</sup>	13 <sup>th</sup>	14 <sup>th</sup>	15 <sup>th</sup>	17 <sup>th</sup>	18 <sup>th</sup>	19 <sup>th</sup>	20 <sup>th</sup>	21 <sup>st</sup>	22 <sup>nd</sup>	25 <sup>th</sup>	30 <sup>th</sup>	31 <sup>st</sup>	32 <sup>nd</sup>	33 <sup>rd</sup>
No of WT	1	1	1	1	4	1	1	1	1	1	6	9	1	2	1
pf(%)	95	95	95	95		95	95	95	95	95			95	95	95
V(%)					101						99.5	100			
PCWT											x	x			

Figure 3(a) indicates the voltage profile in the distribution grid before and after installing 32 WTs. By installing WTs as Table 1, the voltage profile in the grid is improved significantly. At the 18<sup>th</sup> node, before installing WTs, the voltage is only around 91.5% of 12.66 kV, it is lower than the allowable operation range (95-105%); however, after installing 32 WTs, it increases to 101%. Likely, many nodes including the 7<sup>th</sup> to 17<sup>th</sup> nodes and the 26<sup>th</sup> to 33<sup>rd</sup> nodes, the voltage data increases from below 95% to over 99% of 12.66 kV. Generally, nodes' voltage is almost from 99% to 101% and it is in the allowable operation range.

Concerning the power loss on lines, by installing 32 WTs as Table 1, the active power loss on branches is reduced significantly as shown in Figure 3(b). Clearly, on lines near the source, the power loss is reduced significantly from several ten kW to below than 3 kW, taking the line from the 2<sup>nd</sup> node to the 3<sup>rd</sup> node for an example. However, on the 16<sup>th</sup> line which is connected from the 16<sup>th</sup> node to the 17<sup>th</sup> node, the power loss is higher than that before installing WTs because the power flows from the 17<sup>th</sup> node to the 16<sup>th</sup> node to supply the load at the 16<sup>th</sup> node. The active power loss in total is reduced from 202.68 to 18.04 kW.



(a)



(b)

Figure 3. Comparing the performance of the original IEEE 33 bus distribution grid without wind turbine installation to that with 32 WT installation (a) voltage at nodes and (b) power loss on lines

Table 2. Location, operation mode and type of WT in the original IEEE 33-bus distribution grid

Order	Node	Mode		$\Delta P$ (kW)	$V_{min}$ (%)	Order	Node	Mode		$\Delta P$ (kW)	$V_{min}$ (%)	Order	Node	Mode		$\Delta P$ (kW)	$V_{min}$ (%)
		Pf (%)	V (%)					Pf (%)	V (%)					Pf (%)	V (%)		
1 <sup>st</sup>	18	95		186.34	91.9	12 <sup>th</sup>	30	95		72.58	95	23 <sup>rd</sup>	25	99		25.80	95
2 <sup>nd</sup>	33	95		171.54	92.5	13 <sup>th</sup>	11	95		66.82	95	24 <sup>th</sup>	30	99		23.94	95
3 <sup>rd</sup>	17	95		157.89	92.6	14 <sup>th</sup>	17		98	60.67	95	25 <sup>th</sup>	25	99.5		22.11	95
4 <sup>th</sup>	32	95		144.88	93.2	15 <sup>th</sup>	30	95		56.75	95	26 <sup>th</sup>	30	99.5		21.20	95
5 <sup>th</sup>	32	95		133.12	93.7	16 <sup>th</sup>	25	95		53.01	95	27 <sup>th</sup>	22	95		20.46	95
6 <sup>th</sup>	15	95		122.08	93.9	17 <sup>th</sup>	25	95		49.70	95	28 <sup>th</sup>	21	95		20.08	95
7 <sup>th</sup>	31	95		111.92	94.4	18 <sup>th</sup>	17		99	46.45	95	29 <sup>th</sup>	17		101	19.76	95
8 <sup>th</sup>	14	95		102.73	94.6	19 <sup>th</sup>	25		98.5	42.19	95	30 <sup>th</sup>	30		100	18.81	95
9 <sup>th</sup>	30	95		94.05	95	20 <sup>th</sup>	30		98	32.08	95	31 <sup>st</sup>	20	95		18.71	95
10 <sup>th</sup>	30	95		86.25	95	21 <sup>st</sup>	25	95		30.89	95	32 <sup>nd</sup>	19	95		18.70	95
11 <sup>th</sup>	13	95		79.14	95	22 <sup>nd</sup>	30		98.5	27.44	95						

As above results, we obtain PLM when we install 32 WTs. However, if the investment is low, we can install a few WTs as Table 2 indicates the priority order of WT installation. It is noted that the operation mode of WTs at the  $i^{th}$  node is decided by the newest operation mode or the nearest priority order. For example, we only invest 15 WTs; and according to this table, we suggest as following: we install 4 WTs at the 30<sup>th</sup> node, 2 WTs at the 17<sup>th</sup> and 32<sup>nd</sup> node, 1 WT at each node including the 3<sup>rd</sup>, 11<sup>th</sup>, 13<sup>th</sup>, 14<sup>th</sup>, 15<sup>th</sup>, 18<sup>th</sup>, and 31<sup>st</sup> nodes; only WTs at the 17<sup>th</sup> node operates to remain 98% of the rated voltage whereas WTs at other nodes must generate at 95% power factor; the power loss in this grid after installing 15 WTs is reduced from 202.68 to 56.75 kW. Moreover, it is important to note that in this distribution grid, before WTs' installation, the voltage at the 7<sup>th</sup>-18<sup>th</sup> nodes and the 26<sup>th</sup>-33<sup>rd</sup> nodes are normally below 95%, hence, if we install a few WTs, the voltage at these nodes cannot be improved significantly although the power loss is reduced. Hence, we must install up to the 9<sup>th</sup> WT, the voltage at all nodes can satisfy the allowable range.

In comparison to other methods in [4], [5], with the proposed algorithm, the power loss is far lower than that with others although DGs' capacity in total is quite similar. With the proposed algorithm, the power loss is reduced to 18.70 kW by installing 3,200 kW of WT whereas with the methods in [4], [5], the power loss still remains quite high, 72.85 and 51.5 kW by installing 3,040 and 3,111 kW (3,660 kVA/pf=0.85) of DG, respectively. The last column in Table 3 indicates that with the proposed algorithm, the percentage of loss reduction is highest 90.77% whereas they are 75.59% and 65.3% for algorithms in [4], [5], respectively. To compare the efficiency of WT installation, we calculate the percentage of loss reduction per 1 kW of generator. As the last column of Table 3, with the proposed method, this data is 0.0283%/kW while others are below 0.025%/kW. Obviously, the efficiency of the proposed method is higher than that of other methods. Obviously, with the proposed algorithm, we can determine the number and position of WTs to obtain PLM of a radial distribution grid. Results also indicate OOM and the type of WTs.

Table 3. Comparison proposed algorithm and other algorithms

Algorithms	Location	Total	Power loss kW	% Loss reduction
Proposed algorithm		3200	18.70	90.77%(0.0283%/kW)
Algorithm [4]	6,15	(3070+590) kVA/0.85	51.5	75.59%(0.0243%/kW)
Algorithm [5]	13, 30, 24	3040	72.85	65.3%(0.0215%/kW)

**3.2. Modified IEEE 33 bus distribution grid**

The objective of this section is to test a distribution grid where is connected to the power system via multi-nodes. Hence, we suppose that the IEEE 33 bus distribution grid is connected to the power system via three nodes including the 1<sup>st</sup>, 18<sup>th</sup>, and 33<sup>rd</sup> nodes as Figure 2. These nodes are called source nodes and they are operated as swing buses. By running the proposed algorithm, we obtained results as Table 4.

Table 4. Location, operation mode and type of WT in the modified IEEE 33 bus distribution grid

Node	2 <sup>nd</sup>	7 <sup>th</sup>	9 <sup>th</sup>	13 <sup>th</sup>	14 <sup>th</sup>	16 <sup>th</sup>	17 <sup>th</sup>	20 <sup>th</sup>	21 <sup>st</sup>	22 <sup>nd</sup>	24 <sup>th</sup>	25 <sup>th</sup>	27 <sup>th</sup>	29 <sup>th</sup>	30 <sup>th</sup>	31 <sup>st</sup>
No of WT	1	2	5	1	1	1	1	1	1	1	4	6	1	6	1	1
pf (%)	95	95	95	95	95	95			95	95		95	95		95	95
V (%)							1	1			1			1		
PCWT							x	x			x			x		

As can be seen from Table 4, to get PLM in this distribution grid, we need to install 34 WT's at 16 nodes. The 25<sup>th</sup> and 29<sup>th</sup> nodes are required to install the highest number of WT's, 6 WT's for each node. The 9<sup>th</sup>, 24<sup>th</sup>, and 7<sup>th</sup> nodes are also required 5, 4, and 2 WT's, respectively. At other nodes including the 2<sup>nd</sup>, 13<sup>th</sup>, 14<sup>th</sup>, 16<sup>th</sup>, 17<sup>th</sup>, 20<sup>th</sup>, 21<sup>st</sup>, 22<sup>nd</sup>, 27<sup>th</sup>, 30<sup>th</sup>, and 31<sup>st</sup> nodes, we only install one WT at each node. Almost all WT's at nodes are recommended to operate at 95% power factor except WT's at the 17<sup>th</sup>, 20<sup>th</sup>, 24<sup>th</sup>, and 29<sup>th</sup> nodes which are operated in CVM, 100% of the rated value. Moreover, only WT's at the 20<sup>th</sup>, 24<sup>th</sup>, and 29<sup>th</sup> nodes are required to employ PCWT while at other nodes, either PCWT or FCWT can be employed. The total power loss in this grid after installing 34 WT's is 4.048 kW, it cut off 43.676 kW.

Figure 4(a) shows all nodes' voltage before and after installing WT's. Obviously, before installing WT's, the nodes' voltage is in the allowable range (95-105% of the rated value) and it is improved significantly after installing WT's. In fact, before installing 34 WT's, the voltage at the 8<sup>th</sup> to 12<sup>th</sup> and 24<sup>th</sup> to 30<sup>th</sup> nodes is quite low, below 98.5%, but after installing 34 WT's, they are approximately to the rated value. This can be explained by the following reasons. Firstly, installing WT's at many nodes to directly supply the local load leads to reduce the power flow on lines, and hence, the voltage loss on lines is reduced. Secondly, some WT's are operated in CVM to retain the rated voltage at the connected node, and as a result, the voltage at vicinity nodes are improved.

Beside the voltage loss on lines, the power loss on lines is also reduced significantly as Figure 4(b). Obviously, because many WT's are connected to the 9<sup>th</sup> and 29<sup>th</sup> nodes, it makes the power flow on the 8<sup>th</sup> line and the 29<sup>th</sup> line higher than that of without WT, the power loss on these lines becomes higher. However, before connecting WT's, the power loss on the second line is over 12 kW but after installing 34 WT's, it is reduced to below 0.5 kW and this is also seen at many lines such as the 1<sup>st</sup>, 16<sup>th</sup>, from 23<sup>rd</sup>, and 30<sup>th</sup> lines. The main reason is that WT's supply directly power to the local load and it makes the power flow on lines decrease. Consequently, the power loss in total is reduced from 47.72 to 4.05 kW.

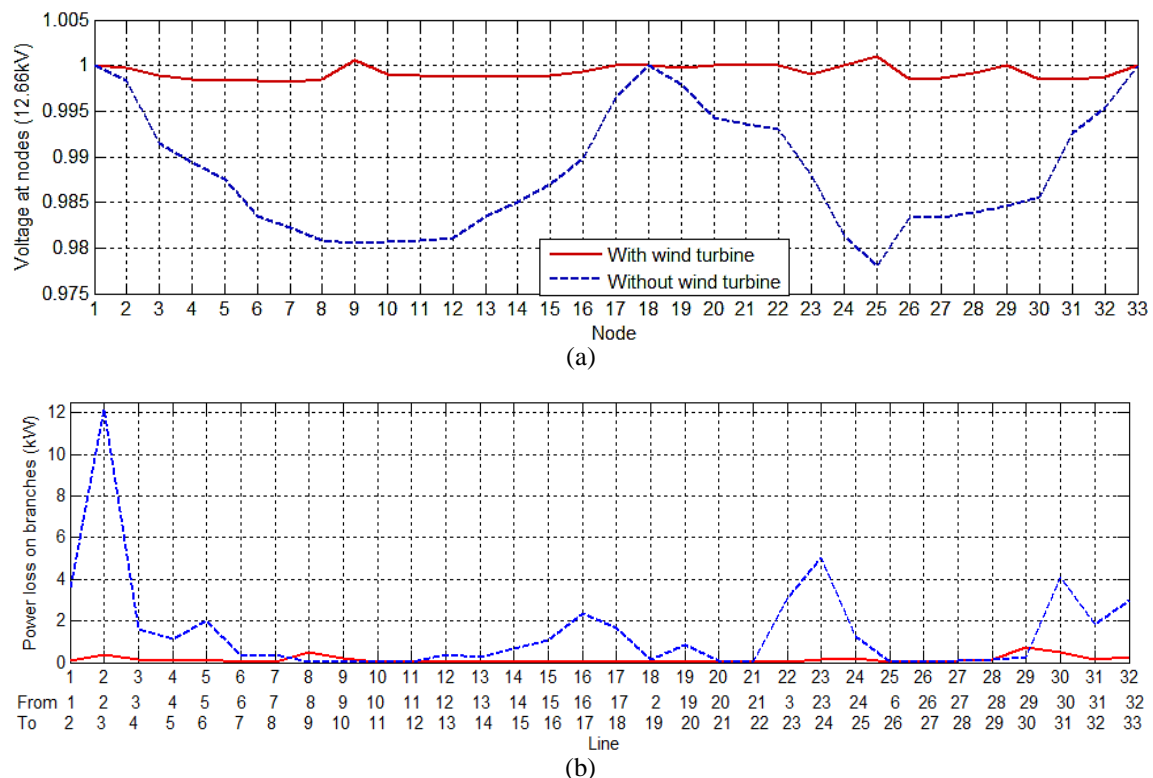


Figure 4. Comparing the performance of the modified IEEE 33 bus distribution grid without wind turbine installation to that with 32 WT installation (a) voltage at nodes and (b) power loss on lines

The priority order of WT installation is indicated in Table 5. The principle of determining the operation mode of WT's at the  $i^{th}$  node up to the  $k^{th}$  order is likely to the Table 4. As can be seen from this table, the 25<sup>th</sup> node is firstly prioritized because it is quite far from swing nodes and its load power is highest; the first 3 WT's are prioritized to connect to the 25<sup>th</sup> node; the next 2 WT's should install at the 9<sup>th</sup> node and so on.

Table 5. The priority order of WT installation in the modified IEEE 33 bus distribution grid

Order	Node	Mode		$\Delta P$ (kW)	Order	Node	Mode		$\Delta P$ (kW)	Order	Node	Mode		$\Delta P$ (kW)
		Pf (%)	Pf (%)				Pf (%)	V (%)				Pf (%)	V (%)	
1 <sup>st</sup>	25	95		43.97	12 <sup>th</sup>	25		99.5	18.20	23 <sup>rd</sup>	14	95		7.04
2 <sup>nd</sup>	25	95		40.67	13 <sup>th</sup>	29		99	16.40	24 <sup>th</sup>	25	95		6.72
3 <sup>rd</sup>	25		98.5	37.45	14 <sup>th</sup>	9	95		15.48	25 <sup>th</sup>	24	95		6.35
4 <sup>th</sup>	9	95		34.74	15 <sup>th</sup>	29	95		14.53	26 <sup>th</sup>	24		100	5.90
5 <sup>th</sup>	9		98.5	32.23	16 <sup>th</sup>	7	95		13.27	27 <sup>th</sup>	20		100	5.76
6 <sup>th</sup>	25	95		29.96	17 <sup>th</sup>	13	95		12.17	28 <sup>th</sup>	16	95		5.64
7 <sup>th</sup>	9	95		27.68	18 <sup>th</sup>	27	95		11.20	29 <sup>th</sup>	18	95		5.62
8 <sup>th</sup>	9		99	24.81	19 <sup>th</sup>	7	95		11.09	30 <sup>th</sup>	17		100	5.61
9 <sup>th</sup>	24		99	22.70	20 <sup>th</sup>	29		99.5	10.40	31 <sup>st</sup>	29	95		5.58
10 <sup>th</sup>	29	95		21.39	21 <sup>st</sup>	22	95		7.86	32 <sup>nd</sup>	30	95		5.29
11 <sup>th</sup>	24	95		20.18	22 <sup>nd</sup>	21	95		7.45	33 <sup>rd</sup>	31	95		5.10
										34 <sup>th</sup>	29		100	4.05

#### 4. CONCLUSION

This paper presents an algorithm to determine the optimal number of WTs such that the power loss in a distribution grid becomes minimum. Beside the optimal number of WTs, this algorithm also determines the optimal location, OOM and the type of WTs. This algorithm was verified via the IEEE 33 bus distribution grid and its modification. Results indicated that the algorithm could give better results than that of other algorithms.

#### ACKNOWLEDGMENT

This work was supported by The University of Danang, University of Science and Technology, code number of project: T2022-02-07.

#### REFERENCES

- [1] Global Wind Energy Council (GWEC), "Global wind energy report 2021," 2021. Accessed: Dec. 01, 2021. [Online]. Available: <https://gwec.net/wp-content/uploads/2021/03/GWEC-Global-Wind-Report-2021.pdf>.
- [2] "Wind turbine grid connection and interaction." ENERGIE, pp. 1–29, Accessed: Dec. 04, 2021. [Online]. Available: [https://ec.europa.eu/energy/sites/ener/files/documents/2001\\_fp5\\_brochure\\_energy\\_env.pdf](https://ec.europa.eu/energy/sites/ener/files/documents/2001_fp5_brochure_energy_env.pdf).
- [3] C. Ma, J.-H. Menke, J. Dasenbrock, M. Braun, M. Haslbeck, and K.-H. Schmid, "Evaluation of energy losses in low voltage distribution grids with high penetration of distributed generation," *Applied Energy*, vol. 256, Dec. 2019, doi: 10.1016/j.apenergy.2019.113907.
- [4] A. Tah and D. Das, "Novel analytical method for the placement and sizing of distributed generation unit on distribution networks with and without considering P and PQV buses," *International Journal of Electrical Power and Energy Systems*, vol. 78, pp. 401–413, Jun. 2016, doi: 10.1016/j.ijepes.2015.12.009.
- [5] E. Karunarathne, J. Pasupuleti, J. Ekanayake, and D. Almeida, "The optimal placement and sizing of distributed generation in an active distribution network with several soft open points," *Energies*, vol. 14, no. 4, Feb. 2021, doi: 10.3390/en14041084.
- [6] K. Mahmoud, N. Yorino, and A. Ahmed, "Power loss minimization in distribution systems using multiple distributed generations," *IEEE Transactions on Electrical and Electronic Engineering*, vol. 10, no. 5, pp. 521–526, Sep. 2015, doi: 10.1002/tee.22115.
- [7] E. Karunarathne, J. Pasupuleti, J. Ekanayake, and D. Almeida, "Optimal placement and sizing of DGs in distribution networks using MLPPO algorithm," *Energies*, vol. 13, no. 23, Nov. 2020, doi: 10.3390/en13236185.
- [8] M. C. V Suresh and E. J. Belwin, "Optimal DG placement for benefit maximization in distribution networks by using Dragonfly algorithm," *Renewables: Wind, Water, and Solar*, vol. 5, no. 1, Dec. 2018, doi: 10.1186/s40807-018-0050-7.
- [9] Y. Merzoug, B. Abdelkrim, and B. Larbi, "Optimal placement of wind turbine in a radial distribution network using PSO method," *International Journal of Power Electronics and Drive Systems (IJPEDS)*, vol. 11, no. 2, pp. 1074–1081, Jun. 2020, doi: 10.11591/ijpeds.v11.i2.pp1074-1081.
- [10] M. Pesarani H.A., P. D. Huy, and V. K. Ramachandaramurthy, "A review of the optimal allocation of distributed generation: Objectives, constraints, methods, and algorithms," *Renewable and Sustainable Energy Reviews*, vol. 75, pp. 293–312, Aug. 2017, doi: 10.1016/j.rser.2016.10.071.
- [11] V. Kalkhambkar, B. Rawat, R. Kumar, and R. Bhakar, "Optimal allocation of renewable energy sources for energy loss minimization," *Journal of Electrical Systems*, vol. 13, no. 1, pp. 115–130, 2017.
- [12] A. Raj, N. F. A. Aziz, Z. M. Yasin, and N. A. Salim, "Investigation of distributed generation units placement and sizing based on voltage stability condition indicator (VSCI)," *International Journal of Power Electronics and Drive Systems (IJPEDS)*, vol. 10, no. 3, pp. 1317–1323, Sep. 2019, doi: 10.11591/ijpeds.v10.i3.pp1317-1323.
- [13] K. Mahmoud and M. Lehtonen, "Simultaneous allocation of multi-type distributed generations and capacitors using generic analytical expressions," *IEEE Access*, vol. 7, pp. 182701–182710, 2019, doi: 10.1109/ACCESS.2019.2960152.
- [14] R. K. Samala and M. R. Kotapuri, "Optimal allocation of distributed generations using hybrid technique with fuzzy logic controller radial distribution system," *SN Applied Sciences*, vol. 2, no. 2, Feb. 2020, doi: 10.1007/s42452-020-1957-3.
- [15] U. Sultana, A. B. Khairuddin, M. M. Aman, A. S. Mokhtar, and N. Zareen, "A review of optimum DG placement based on minimization of power losses and voltage stability enhancement of distribution system," *Renewable and Sustainable Energy Reviews*, vol. 63, pp. 363–378, Sep. 2016, doi: 10.1016/j.rser.2016.05.056.
- [16] V. S. Galgali, M. Ramachandran, and G. A. Vaidya, "Multi-objective optimal sizing of distributed generation by application of

- Taguchi desirability function analysis,” *SN Applied Sciences*, vol. 1, no. 7, Jul. 2019, doi: 10.1007/s42452-019-0738-3.
- [17] B. Saleh, L. J. Yin, and R. Verayiah, “Voltage regulation and power loss reduction by integration of SVC in distribution networks via PSSSE,” *International Journal of Power Electronics and Drive Systems (IJPEDS)*, vol. 11, no. 3, pp. 1579–1587, Sep. 2020, doi: 10.11591/ijped.v11.i3.pp1579-1587.
- [18] A. Sadighmanesh, K. Zare, and M. Sabahi, “Distributed generation unit and capacitor placement for multi-objective optimization,” *International Journal of Electrical and Computer Engineering (IJECE)*, vol. 2, no. 5, Oct. 2012, doi: 10.11591/ijece.v2i5.1590.
- [19] M. H. Ali, M. Mehanna, and E. Othman, “Optimal planning of RDGs in electrical distribution networks using hybrid SAPSO algorithm,” *International Journal of Electrical and Computer Engineering (IJECE)*, vol. 10, no. 6, pp. 6153–6163, 2020, doi: 10.11591/ijece.v10i6.pp6153-6163.
- [20] J. P. Sridhar and R. Prakash, “Multi-objective whale optimization based minimization of loss, maximization of voltage stability considering cost of DG for optimal sizing and placement of DG,” *International Journal of Electrical and Computer Engineering (IJECE)*, vol. 9, no. 2, pp. 835–839, Apr. 2019, doi: 10.11591/ijece.v9i2.pp835-839.
- [21] B. Wu, Y. Lang, N. Zargari, and S. Kouro, *Power conversion and control of wind energy systems*. Hoboken, NJ, USA: John Wiley & Sons, Inc., 2011.
- [22] P. D. Chung, “Evaluation of reactive power support capability of wind turbines,” *Engineering, Technology and Applied Science Research*, vol. 10, no. 1, pp. 5211–5216, Feb. 2020, doi: 10.48084/etasr.3260.
- [23] M. Tsili and S. Papanthassiou, “A review of grid code technical requirements for wind farms,” *IET Renewable Power Generation*, vol. 3, no. 3, 2009, doi: 10.1049/iet-rpg.2008.0070.
- [24] M. R. M. Cruz, D. Z. Fitiwi, S. F. Santos, and J. P. S. Catalao, “Influence of distributed storage systems and network switching/reinforcement on RES-based DG integration level,” in *2016 13th International Conference on the European Energy Market (EEM)*, Jun. 2016, pp. 1–5, doi: 10.1109/EEM.2016.7521337.
- [25] E. Möllerström, P. Gipe, J. Beurskens, and F. Ottermo, “A historical review of vertical axis wind turbines rated 100 kW and above,” *Renewable and Sustainable Energy Reviews*, vol. 105, pp. 1–13, May 2019, doi: 10.1016/j.rser.2018.12.022.
- [26] M. M. Rezaei, “A nonlinear maximum power point tracking technique for DFIG-based wind energy conversion systems,” *Engineering Science and Technology, an International Journal*, vol. 21, no. 5, pp. 901–908, Oct. 2018, doi: 10.1016/j.jestch.2018.07.005.

## BIOGRAPHIES OF AUTHORS



**Dinh Chung Phan**    has been a lecture at Faculty of Electrical engineering, The university of Danang-University of Science and Technology in Vietnam since 2004. He obtained Engineering Degree, master’s degree, and philosophy degree in electrical engineering from the university of Danang-University of Science and Technology in 2004, Dongguk university in Korea in 2011, and Kanazawa university in Japan in 2017, respectively. His research activities are in fields of renewable energy, power systems, and control. He can be contacted at pdchung@dut.udn.vn. Further info on his homepage: <http://scv.udn.vn/phandinhchung>.



**Ngoc An Luu**    has been a lecture at Faculty of Electrical Engineering, The University of Danang-University of Science and Technology in Vietnam since 2005. He obtained Engineering Degree, master’s degree, and philosophy degree in Electrical Engineering from The University of Danang-University of Science and Technology in 2004, National Cheng Kung University in Taiwan in 2010, and Grenoble Institute of Technology in France in 2014, respectively. His research activities are in the fields of renewable energy, power systems, and energy management. He can be contacted at lnan@dut.udn.vn. Further info on his homepage: <http://scv.udn.vn/lungocan>.